Simple and approximate upper-limit estimation of future precipitation return-values

R. E. Benestad[1], K. M. Parding[1], A. Mezghani[1], A. V. Dyrrdal[1]

[1]The Norwegian Meteorological Institute, Oslo, 0313, Norway

Correspondence to: Rasmus E. Benestad (rasmus.benestad@met.no)

Abstract. We present estimates for an upper limit for twenty-year return-values for 24-hr precipitation at different locations in Europe and a crude method to quantify bounds of likely intervals. Our results suggest an increase by as much as 40-50% projected for 2100, assuming a high emission scenario, RCP8.5. The new strategy is based on combining physics with the limited available information, and utilises the covariance between the mean seasonal variations in precipitation and the North Atlantic saturation vapour pressure to estimate the maximum effect that a temperature change can have on precipitation, rather than the actual expected values. Return-value projections were derived through a simple and approximate scheme that combines the one-year 24-hr precipitation return-value and downscaled annual wet-day mean precipitation for a 1-in-20 year event. The twenty-year return-value was estimated by the 95th percentile of multi-model ensemble spread of downscaled climate model results. We found geographical variations in the shape of the seasonal cycle of the wet-day mean precipitation which suggest that different rain-producing mechanisms dominate in different regions. These differences indicate that the simple method used here to estimate upper limits was more appropriate for convective precipitation than for orographic rainfall.

1 Introduction

Extreme precipitation is associated with flooding and landslides and can have detrimental effects on infrastructure and society (Trenberth et al, 2003), as for example during the unusually intense cloudburst in central Copenhagen on July 2, 2011 which caused massive flooding, and the 2002 floods in central and eastern Europe (Hov et al., 2013). Return-values are commonly used in planning and design of weather-resilient infrastructure by quantifying the magnitude of a typical extreme event. However, the return-values are not stationary, and according to the insurance company Munich Re (Hov et al., 2013), there has been an increase in the annual number of loss-relevant weather events. Assessments carried out by the Intergovernmental Panel on Climate Change (IPCC) indicate that heavy precipitation will become more severe in already wet areas in the future (Stocker et al., 2013, Field et al, 2012). These assessments have largely been based on global climate model (GCM) output and have not made use of additional local information such as observations. One of the difficulties of using observational data is the patchy character of the information because of missing data and short records. GCMs are not designed to represent local precipitation statistics corresponding to rain gauge data, but are expected to reproduce the nature

of large-scale (regional and global) phenomena and processes seen in the atmosphere and oceans. Also, some elements are reproduced with higher skill than others. In other words, GCMs provide a more reliable picture of the temperature aggregated over larger spatial scales than grid-box precipitation estimates (Takayabu et al., 2016), and their ability to simulate large-scale features can be utilised for inferring changes to local precipitation through downscaling (Benestad et al, 2008). This caveat also applies to regional climate models (RCMs), which too have a minimum skillful scale (Takayabu et al., 2016), and have a limited ability to reproduce the observed precipitation statistics (Orskaug et al., 20122; Benestad and Haugen, 2007). However, RCMs have been used to study precipitation extremes (e.g. Frei et al., 2006). The use of RCMs are limited to a small number of GCMs due to their heavy computational demands, which means that they will not provide a realistic range of possible outcomes, e.g. associated with natural variability (Deser et al., 2012). Traditional methods of estimating return-values that make use of the extreme value theory (EVT) are sensitive to sampling fluctuations and require long data records to avoid extrapolation of the extreme characteristics (Coles, 2001; Papalexiou and Koutsoyiannis, 2013). Extreme precipitation modelled through EVT usually describes amounts that are far out in the tail of the distribution and associated with low probability, and the estimates may change when new extremes are sampled. Most uses of EVT also assume stationarity, although there are ways to account for trends (Cheng et al., 2014).

There are many different types of phenomena that generate precipitation, e.g., the formation of stratonimbus, mid-latitude cyclones, fronts, atmospheric rivers, and convection, as well as warm and cold initiation of rain (Fleagle and Businger, 1980; Berg et al., 2012; Trenberth et al., 2003). Some of these are more strongly present in certain regions and seasons. For instance, convective precipitation is typically a summer phenomenon at mid-to-high latitudes, whereas mid-latitude cyclones are more pronounced in autumn, winter, and spring. Daily local precipitation has been notoriously difficult to predict (Stocker, 2013; Field et al. 2012; Arkin et al., 1994), and one reason may be that it has involved a blend of different (both dry and wet days) conditions and phenomena but subject to the same analysis without accounting for these differences (e.g. monthly mean precipitation mixes wet and dry days). Another reason may be that quantities such as the monthly mean values are poorly estimated due to small real samples for locations where it rains less than 30% of the total number of days.

The problem concerning the quantification of future extreme precipitation is associated with uncertainties from a number of sources, many of which are connected with methods and may include model imperfections, sparsity of data, sensitivity to random variations in small samples such as the tail of the distribution, non-stationarities, and representation of natural variability. The latter point may to some extent be explored through the use of large multi-GCM ensembles, however, it is interesting to explore extremes from a different angle by posing the research question in the following way: *Is it possible to extract robust information about extreme precipitation from the multitude of data sources available?* Or more specifically, *is it possible to estimate the* ***upper limits*** *of change in extreme precipitation amounts associated with increased temperature, rather than the most likely value, using the available local information in combination with the output of GCM ensembles?*

2 Data and Method

Our objective is to get robust estimates of future extreme precipitation in situations when local observations are limited and avoid some of the caveats described above. Our approach was based on empirical-statistical downscaling (ESD) applied to an ensemble distribution to provide estimates of upper limits to return-values for heavy precipitation, and is an alternative to EVT-based approaches. It provides more approximate and cruder, but more robust estimates because a larger portion of the data sample is used and it is not as sensitive to sampling fluctuations which make small sample statistics highly uncertain. Furthermore, it differs from traditional methods in that it estimates upper bounds of extreme precipitation, rather than attempting to specify the most likely values. The analysis draws on available and relevant information concerning precipitation, for instance geographical variations, seasonal variations, ensemble spread, and different physical processes present during wet and dry days, respectively. The supporting material (SM) provides more details and explanations for why we chose the particular strategy for inferring changes in the upper limits to return values for precipitation due to a temperature change.

2.1 Data

Precipitation observations were obtained from the daily ECA&D dataset (Klein Tank et al., 2002) for 1032 stations in northern Europe with data available for the time period 1961-2014 (Figure 2). Surface temperature data from the NCEP/NCAR reanalysis 1 (Kalnay et al, 1996) over the North Atlantic domain were used as predictors in the downscaling, and corresponding projections from the CMIP5 ensembles of GCMs assuming the RCP 2.6, 4.5, and 8.5 scenarios (Taylor et al, 2011) were used for the projections of future change (Table 1).

2.2 Downscaling method

2.2.1 Predictand: the wet-day mean precipitation

Moderate extremes in 24-precipitation amount can be approximated with an exponential distribution (Benestad et al, 2012a,b, Benestad, 2013), which is described with one parameter - the wet-day mean μ. The exponential distribution can be used to estimate changes in the moderate upper tail of the statistical distribution, assuming that these follow changes in the bulk characteristics where the probability adds up to unity (Benestad and Mezghani, 2015). It simplifies the analysis and can be used to provide an estimate of return-values for more extreme extremes if its parameter is derived from years with high annual wet-day mean precipitation. In other words, making use of conditional probabilities à la the type of Bayesian statistics described in Benestad et al. (2012b), which makes the strategy well-suited to address the question of how we can quantify changes in the return-values associated with a global warming.

We explored the sensitivity of μ to changing factors. The wet-day mean μ, rather than the mean precipitation ($\overline{x}$), was downscaled, because μ provides a 'cleaner' representation of the typical precipitation amount. A comparison between the seasonal dependence of the traditional mean precipitation, wet-day frequency f_w, and μ indicates a stronger seasonal cycle in

μ than in $\bar{x}$ or f_w. The difference in the seasonal cycle is due to the blending of different types of weather conditions in the traditional mean. The wet-day mean precipitation is useful for risk analysis; previous work suggests that it can be used to estimate upper percentiles of 24-hr precipitation amounts since wet-day 24-hr precipitation is approximately exponentially distributed for low to moderately heavy precipitation amounts, implying that the wet-day 95-percentile is expected to change in proportion with the wet-day mean (Benestad et al, 2012a,b, Benestad, 2013; Benestad and Mezghani, 2015).

2.2.2 Predictor: the saturation vapour pressure

We assumed that the vapour saturation pressure, e_s, is more linearly related to the atmospheric water content and precipitation than is temperature, and hence used e_s as a predictor in the downscaling of μ (Fujibe, 2013; Pall et al., 2007; Benestad and Mezghani, 2015). The saturation vapour pressure was estimated from the surface temperature, T, according to $e_s = 10^{(11.40-2353/T)}$. This approximation was based on integration of the Clausius-Capeyron equation, assuming a constant latent heat of vaporisation (see Equation 2.89 in Fleagle and Businger, 1980).

The regional average e_s over the North Atlantic domain (100°W-30°E/0°N-40°N) was used as predictor of μ with the motivation that it can be considered a source region for humidity in Europe. The predictor index was calculated from gridded temperature data from reanalyses and global climate models (GCMs) and then spatially and temporally aggregated, where monthly gridded e_s values from the multi-model ensemble were used to produce (downscale) an ensemble of local results of μ.

2.2.3 The empirical-statistical model

A model for predicting the wet-day mean precipitation (the prediction for the wet-day mean is referred to as , whereas the original wet-day mean is just μ) can be constructed as a sum of a constant β_0, a term depending on the saturation vapour pressure $\beta_T e_s$, and a Gaussian noise term $N(0,\sigma)$, assuming that factors other than temperature affecting wet-day precipitation are stochastic and stationary:

$$\hat{\mu} = \beta_0 + \beta_T e_s + N(0,\sigma) \quad , \qquad (1)$$

As an estimate of the standard deviation σ of the noise term N, we used the observed standard deviation of μ in the month with the highest inter-annual variability, which in this case is August. We used R^2 to quantify the ratio explained variation (var($\hat{\mu}$) with the noise term is taken to be zero) to the total variation (var(μ)). The assumption that only e_s influences precipitation is often not true, and hence the model represented an upper-limit approximation of the effect that temperature changes can have on μ, rather than a most likely value.

Different downscaling models (Equation 1) were derived for each location based on a regression between the monthly mean seasonal cycle of μ (see section 2.2.1) and the corresponding mean seasonal cycle of the regionally averaged North Atlantic

e_s (section 2.2.2) calculated from reanalysis temperature data. Annual mean time series of μ were then derived by applying the downscaling models to annual mean e_s time series obtained from reanalysis or GCM temperature data.

A 90% confidence interval for the upper limit estimates was estimated for the projections based on both the ensembles of downscaled results as well as the noise term *N(0,)*, taken as the limit between the 5th and 95th percentiles (e.g Figure SM11 in the SM). This interval captured the observed year-to-year variations as well as model differences, as internal nondeterministic interannual-to-decadal variations account for much of observed variability as well as differences between climate model simulations (Deser et al., 2012). We assumed that the multi-model ensemble spread for any given year could approximately represent the typical year-to-year variance, and hence the 95th percentile for the annual wet-day mean precipitation $\hat{\mu}$ was used as a proxy for the value to be exceeded once in 20 years on average (Benestad, 2011).

2.3 Return-value probabilities

We replaced the general mean μ' with the 20-year return-value for the mean $\hat{\mu}$, and the probability for 24-hr precipitation exceeding a critical threshold x was calculated based on the assumption that the wet-day precipitation-amount is exponentially distributed:

$$f\left(X>x\right)=f_w e^{-x/\mu} \quad , \qquad (2)$$

The probability for the one-year return-value for 24-hr precipitation is approximately Pr(X > x) = 1/365.25, and for data that are close to being exponentially distributed, the corresponding threshold value can be approximated according to:

$$x_{1\text{year}}=\mu' \ln\left(365.25 * f_w\right) \quad , \qquad (3)$$

If the return-values associated with the 24-hr precipitation are related to the annual wet-day mean, as in Equation 3, then it is possible to make a rough estimate of the 20-year return-value for the 24-hr precipitation amount based on the 20-year return-value for μ'. Previous comparison between the return-values based on Equation 3 and general extreme value theory, suggests that they give roughly similar results (Benestad and Mezghani, 2015). A test of Equation 3 indicates that the return-values scale with μ, and that x_{1year} associated with high quantiles and low values of μ approximately correspond to x_{1year} with low quantiles and high values of μ (Figure SM1). Hence, estimates of the 20-year return-value for 24-hr precipitation can be estimated approximately using Equation 3 and taking μ to be the 95th percentile.

2.4 Principle component analysis of the seasonal cycle

Principal component analysis (PCA) was used to extract the most dominant shapes of the seasonal cycle in μ amongst the locations (Figure 2). The mean seasonal cycle was estimated for each site, taking the calendar month mean, and used to construct a data matrix *X*. Singular value decomposition (SVD) was then used to compute the principal components: $U\Sigma V^T = X$, where *U* is the left inverse, *V* the right inverse, and Σ is a diagonal matrix holding the eigenvalues (Press et al., 1989; Strang, 1988). The procedure deconstructs the data into a set of shapes of the seasonal cycle, corresponding eigenvalues that describe the explained variance, and a spatial matrix that describes the relative strength of each shape at the different

locations. The analysis presented here was carried out with the open-source R-package 'esd' (Benestad et al., 2015), and the R-scripts are provided in the SM.

3 Results and discussion

3.1 Seasonal cycles of μ and es

Our results show that the mean seasonal cycles of μ at many European locations covaries with the mean seasonal cycle of e_s in the North Atlantic domain. This can be seen as a validation of the assumptions underlying the empirical model (Equation 1). Figure 1 provides an example of a scatter plot between the mean seasonal variations in e_s (x-axis) and the corresponding cycle in μ (y-axis) for one location (Velikie Luki, Russia). The example in Figure 1 is not unique: there is a high and statistically significant correlation ($R^2 > 0.6$) between the seasonal cycle of these two quantities for many of the rain gauge records (612 of the 1032 stations; Figure SM2). The majority of the locations with a poor fit ($R^2 < 0.6$) are found along the Norwegian west coast and southeast of the Alps (see Figure 2 where the size of the markers is proportional to R^2), while inland sites and locations in central Europe have higher R^2 values. This indicates that a linear relationship between μ and e_s cannot be expected in regions where orographic precipitation is dominant. Downscaled projections are produced only for the locations with a good fit ($R^2 > 0.6$ corresponding to 65% of the total sample, see Figure SM2).

It is also evident that there are pronounced year-to-year variations in the wet-day mean (vertical error bars in Figure 1) which are not related to the temperature, suggesting that factors other than temperature also play a role in precipitation variations. The downscaling strategy adopted here is designed to evaluate the maximum potential effect of temperature changes on the wet-day mean. Since other processes also influence precipitation, the method cannot be expected to reproduce past interannual variability, but it can be used to obtain a rough estimate of the effect of temperature changes on precipitation.

Figure 2 presents maps showing the two major components of the mean seasonal cycle in μ, which together account for 94% of the variability for the 1032 locations examined. There is a positive correlation between R^2 from the regression analysis (equation 1) and the spatial vector of the leading PC: 0.82 (with 90% confidence interval of 0.80, 0.84), but negative correlation for mode 2 (-0.84; conf. int. -0.86,-0.82) and none for mode 3 (0.00; conf. int. -0.06, 0.06). The spatial patterns in the PCs reveal different seasonal cycles of precipitation along the mountainous western coast of Norway and close to the Alps compared to the rest of Europe, probably related to orographic effects. There is a gradient in the shape of the mean seasonal cycle in μ with the distance from the coast that is particularly visible over the Netherlands. Inland sites tend to indicate higher precipitation intensities during July and August, which can be associated with convective rainfall.

3.2 Projections of future precipitation

Projected values for μ, based on the downscaling model (Equation 1) applied to the CMIP5 ensemble, are shown in Figure 3. The downscaled results suggest an increase of up to 13% in the wet-day mean from 2010 to 2100, assuming the RCP 4.5

emission scenario (Stocker et al, 2013), and as much as 38% at many of the locations given the high emission scenario RCP8.5. The most extreme upper limit estimate is an 85% increase at Sihccajavri (Norway). Since the wet-day precipitation amount approximately follows an exponential distribution, the proportional change in any percentile is the same as for μ. The insert in Figure 3 shows estimated changes for the emission scenarios RCP4.5, RCP2.6 and RCP 8.5, respectively, for both the ensemble mean and 95th percentile.

Historical observations provide some indication of skill of the downscaling models in terms of predicting trends of μ based on the North Atlantic temperature (Figure SM3). The historical trends exhibit a more pronounced scatter than the predicted trends, suggesting that factors other than the sea surface temperature also have influenced the long-term changes. For most locations, there has been an increase in μ between 1961 and 2014, typically ~0.1 mm/day per decade (Figure SM3-4).

Estimates of future 20-year return-values based on the downscaled μ and assuming a constant value the wet-day frequency, f_w, are shown in Table 2: Based on downscaling of the RCP4.5 scenario, the 20-year return values could increase by between 7% and 28% (ensemble median: 11%), or assuming the high emission scenario RCP8.5, between 22% to 85% (ensemble median: 33%). Nevertheless, changes in f_w may also influence the return-values, and an increase in the number of rainy days would imply an even stronger change in return-values. When accounting for the wet-day frequency, the 20-year return-values can be estimated based on the 99-percentile of the wet-day distribution (Figure SM5). The historical f_w trends at the stations tend to cluster roughly around zero (Figure SM6). However, studying the geographical pattern of trends, we see a general increase in southern Scandinavia and the Netherlands, and a less coherent pattern elsewhere (Figure SM7). This further supports the interpretation that factors other than the North Atlantic temperature also play a role for past trends and future changes. In this sense, the estimation strategy represents a "worst-case" precipitation change, taking only the temperature change into consideration. The wet-day frequency is strongly influenced by the circulation patterns (Benestad and Mezghani, 2015) and could potentially be predicted based on the mean sea-level pressure, but here we have focused on the influence of temperature changes on the precipitation.

One relevant question is whether the high-end tail of the wet-day precipitation distribution changes proportionally to the change in more moderate events (Pall et al., 2007). An analysis of past variations suggested that return-values representing the high-end of the tail of the distribution for years with low annual μ changed proportionally to return-values in the moderate parts of the tail for years with high annual μ, as expected for an exponential distribution (Figure SM1). This is an important condition, as our method makes use of the percentiles corresponding to a one-in-a year event (p = 1 - 1/365.25), but replaces the mean value of μ with a one-in-twenty year event based on the 95-percentile of the downscaled ensemble results.

In order to assess the veracity of our results we include an independent test to examine the dependency of μ to temperature. It consisted of a regression analysis comparing the geographical distribution in the seasonal cycles of μ and the saturation vapour pressure e_s calculated from local temperature measurements (Benestad, 2007) (see Figures SM8-9), and was limited

to locations where both temperature and precipitation observations were available. The independent test did not involve the regionally averaged temperature of the North Atlantic domain. The sensitivity of the geographical variations in climatological μ to temperature was consistent with regression coefficients on which the results in Figure 3 were based within the range of estimated error margins (Figure SM9). An exception was (again) seen in stations located in western Norway and south of the Alps with low R^2.

One of the benefits of the proposed strategy for downscaling μ is that the description of the seasonal cycle does not require long data records and hence may provide a means for estimating an upper limit to the change in rainfall statistics associated with a temperature change in regions with limited observations. This strategy can be used for other mid-latitude locations, but further analysis is needed to see if it is applicable to the monsoon regions where the temperature is at maximum before the rains start. An alternative approach could be to estimate future changes in μ based on downscaled local temperature from GCMs and a similar regression model as used in the test.

4 Summary and conclusions

We propose a novel and simple method for estimating an upper limit to changes in the return-values for 24-hr precipitation caused by a temperature change, rather than trying to estimate the exact value taking all precipitation relevant processes into account. This method makes use of the limited available information, embedded in the seasonal cycle, physical conditions, and multi-model ensembles, to provide a rough estimate of the effect a temperature change may have on precipitation statistics. The approach is based on a set of assumptions: (a) the maximum seasonal mean response of μ to the seasonal variations in temperature is represented by a proportional change, (b) the 95-percentile of the annual wet-day mean precipitation from large multi-model ensembles such as those from CMIP can be used to represent a 20-year event, and (c) the wet-day frequency is stationary. On the one hand, this new strategy is less rigorous than traditional extreme value statistics, but on the other hand, it makes the most out of the available information and is thus more robust. The results suggest that the upper bound of the twenty-year return-value for many European locations increases by 40-50% by 2100, given the RCP8.5 scenario.

Acknowledgments and Data

The methods and results produced for this paper were connected to research carried out for the H2020 EU-Circle (GA no 653824), Nordforsk eSACP. The work was supported by the Norwegian Meteorological Institute. The data used are listed in the references, supporting material, tables, supplements and https://github.com/metno/esd_Rmarkdown/tree/master/paper58.

Table 1. Summary of the CMIP5 experiments. The RCP4.5 was used as default here, whereas RCP2.6 and 8.5 were taken as lower and upper limits based on different emission scenarios.

Ensemble	**Total ensemble size (with duplicated models)**
RCP4.5	108 runs
RCP2.6	81 runs
RCP8.5	65 runs

Table 2. Summary of the projected change in the 20-year return-value for 24-hr precipitation under the assumption of stationary wet-day frequency. The sample comprises the 615 locations shown in Figure 3 and provides a concise summary. The numbers represent the change in percentage with respect to year 2010.

	Min.	1st Qu.	Median	Mean	3rd Qu.	Max.
RCP2.6	4%	5%	6%	6%	7%	14%
RCP4.5	7%	10%	11%	13%	15%	28%
RCP8.5	22%	28%	33%	38%	44%	85%

Figure 1. A comparison between the mean seasonal cycle in the saturation vapour pressure (xaxis) and the wet-day mean (y-axis). The error bars indicate two standard deviations of the year-to-year differences in the two variables, and the insert presents standardised values associated with each calendar month, both peaking in July-August.

Figure 2. The weights for the two leading principal components (panels a and b) of the seasonal cycle of the wet-day mean precipitation μ in the 1032 rain gauge records. The colour of the symbols indicate how strongly the shape is present in the local seasonal cycle, and the size reflects R^2 from the regression analysis between e_s and μ (see Figure SM2). The shape of the seasonal cycle principal component for μ is shown in the insert (top right of each panel).

Figure 3. Projected local change from 2010 to 2100 in the ensemble mean and 95th percentile annual mean μ for the RCP4.5 emission scenario. The colour of the inner part of the symbols indicate changes in the ensemble mean and the outer part the 95th percentile in terms of percentages since 2010. The insert shows a boxplot of the projected change in μ, both for the ensemble mean (left) and the 95th percentile (right) of emissions scenarios RCP4.5, RCP2.6, and RCP8.0 respectively.

References

Arkin, P. A., R. Joyce, and J.E. Janowiak. “The Estimation of Global Monthly Mean Rainfall Using Infrared Satellite Data: The GOES Precipitation Index (GPI).” Remote Sensing Reviews 11, no. 1–4 (October 1, 1994): 107–24. doi:10.1080/02757259409532261.

Benestad, R. E., and A. Mezghani. “On Downscaling Probabilities for Heavy 24-Hour Precipitation Events at Seasonal-to-Decadal Scales.” Tellus A 67, no. 0 (March 30, 2015). doi:10.3402/tellusa.v67.25954.

Benestad, R. E. “Association between Trends in Daily Rainfall Percentiles and the Global Mean Temperature.” Journal of Geophysical Research: Atmospheres 118, no. 19 (2013): 10,802–10,810. doi:10.1002/jgrd.50814.

Benestad, R.E., D. Nychka, and L. O. Mearns. “Specification of Wet-Day Daily Rainfall Quantiles from the Mean Value.” Tellus A 64, no. 14981 (2012a). doi:10.3402/tellusa.v64i0.14981.

Benestad, R.E., D. Nychka, and L. O. Mearns. “Spatially and Temporally Consistent Prediction of Heavy Precipitation from Mean Values.” Nature Climate Change 2, no. doi: 10.1038/NCLIMATE1497 (2012b).

Benestad, R.E. “Novel Methods for Inferring Future Changes in Extreme Rainfall over Northern Europe.” Climate Research 34, no. doi: 10.3354/cr00693 (2007): 195–210.

Benestad, R. E. “A New Global Set of Downscaled Temperature Scenarios.” Journal of Climate 24, no. 8 (2011): 2080–98. doi:10.1175/2010JCLI3687.1.

Benestad, R.E. , A. Mezghani, and K.M. Parding. “Esd V1.0,” 2015. doi:10.5281/zenodo.29385.

Benestad, R. E., and J. E. Haugen. “On Complex Extremes: Flood Hazards and Combined High Spring-Time Precipitation and Temperature in Norway.” Climatic Change 85, no. doi:10.1007/s10584-007-9263-2 (2007): 381–406.

Benestad, Rasmus E., Inger Hanssen-Bauer, and Deliang Chen. Empirical-Statistical Downscaling. World Scientific, 2008.

Berg, P., C. Moseley, and J.O. Haerter. “Strong Increase in Convective Precipitation in Response to Higher Temperatures.” Nature Geoscience 6, no. 3 (February 17, 2013): 181–85. doi:10.1038/ngeo1731.

Cheng, Linyin, Amir AghaKouchak, Eric Gilleland, and Richard W. Katz. “Non-Stationary Extreme Value Analysis in a Changing Climate.” Climatic Change 127, no. 2 (September 24, 2014): 353–69. doi:10.1007/s10584-014-1254-5.

Coles, S G., 2001. An Introduction to Statistical Modeling of Extreme values. Springer Series in Statistics.

Deser, C., R. Knutti, S. Solomon, and A. S. Phillips. “Communication of the Role of Natural Variability in Future North American Climate.” Nature Climate Change 2, no. doi:10.1038/nclimate1562 (2012): 775–79.

Field, C.B., V. Barros, T. F. Stocker, D. Qin, D. J. Dokken, K. L. Ebi, M. D. Mastrandrea, et al., eds. Managing the Risks of Extreme Events and Disasters to Advance Climate Change Adaptation. A Special Report of Working Groups I and II of the Intergovernmental Panel on Climate Change. Cambridge, UK, and New York, NY, USA: Cambridge University Press, 2012.

Fleagle, R. G., and J. A. Businger. An Introduction to Atmospheric Physics. 2nd ed. Vol. 25. International Geophysics Series. Orlando: Academic Press, 1980.

Fujibe, F. (2013), Clausius–Clapeyron-like relationship in multidecadal changes of extreme short-term precipitation and temperature in Japan. Atmosph. Sci. Lett., 14: 127–132. doi: 10.1002/asl2.428

Frei, C., R. Schöll, S. Fukutome, J. Schmidli, and P. L. Vidale. "Future Change of Precipitation Extremes in Europe: Intercomparison of Scenarios from Regional Climate Models." Journal of Geophysical Research 111, no. doi:10.1029/2005JD005965 (2006): D06105.

Hov, Ø., C. Cubasch, E. Fischer, P. Höppe, T. Iversen, N.G. Kvamstø, Z.W. Kundzewicz, et al. "Extreme Weather Events in Europe: Preparing for Climate Change Adaptation." MET Norway, The Norwegian Academy of Sciences and Letters (DNVA), European Academies Science Advicery Council (EASAC), 2013.

Jaeger, L. "Monthly and Areal Patterns of Mean Global Precipitation." In Variations in the Global Water Budget, edited by Alayne Street-Perrott, Max Beran, and Robert Ratcliffe, 129–40. Springer Netherlands, 1983. http://link.springer.com/chapter/10.1007/978-94-009-6954-4_9.

Kalnay, E., M. Kanamitsu, R. Kistler, W. Collins, D. Deaven, L. Gandin, M. Iredell, et al. "The NCEP/NCAR 40-Year Reanalysis Project." Bull. Amer. Meteor. Soc. 77 (March 1996): 437–71.

Klein Tank, A.M.G.and J. B. Wijngaard, G. P. Konnen, R. Böhm, G. Demarée, A. Gocheva, M. Mileta, S. Pashiardis, et al. "Daily Dataset of 20th-Century Surface Air Temperature and Precipitation Series for the European Climate Assessment." International Journal of Climatology 22 (2002): 1441–53.

Orskaug, E., I. Scheel, A. Frigessi, : Guttorp, J.E. Haugen, O.E. Tveito, and O. Haug. "Evaluation of a Dynamic Downscaling of Precipitation over the Norwegian Mainland." Tellus 63A (2011): 746–56.

Pall, P., M. R. Allen, and D. A. Stone. "Testing the Clausius–Clapeyron Constraint on Changes in Extreme Precipitation under CO2 Warming." Climate Dynamics 28, no. 4 (January 16, 2007): 351–63. doi:10.1007/s00382-006-0180-2.

Papalexiou, S M, and Koutsoyiannis, D., 2013. Battle of extreme value distributions: A global survey on extreme daily rainfall. Water Resour. Res., 49(1), 187–201.

Press, W. H., B. P. Flannery, S. A. Teukolsky, and W. T. Vetterling. Numerical Recipes in Pascal. Cambridge, UK: Cambridge University Press, 1989.

Stocker, T.F., D. Qin, G.-K. Plattner, M. Tignor, S.K. Allen, J. Boschung, A. Nauels, Y. Xia, V. Bex, and M. Midgley. Climate Change 2013: The Physical Science Basis. Contribution of Working Group I to the Fifth Assessment Report of the Intergovern - Mental Panel on Climate Change. Cambridge, United Kingdom and New York, NY, USA: Cambridge University Pres, 2013.

Strang, G. Linear Algebra and Its Application. San Diego, California, USA: Harcourt Brace & Company, 1988.

Takayabu, I., H. Kanamaru, K. Dairaku, R. Benestad, H. von Storch, and J. Hesselbjerg Christensen. "Reconsidering the Quality and Utility of Downscaling." Journal of the Meteorological Society of Japan. Ser. II 94A, no. 0 (2016): 31–45. doi:10.2151/jmsj.2015-042.

Taylor, K. E., R. J. Stouffer, and G. A. Meehl. "An Overview of CMIP5 and the Experiment Design." Bulletin of the American Meteorological Society 93, no. 4 (October 7, 2011): 485–98. doi:10.1175/BAMS-D-11-00094.1.

Trenberth, K.E. , Aiguo Dai, Roy M. Rasmussen, and David B. Parsons, 2003: The Changing Character of Precipitation. Bull. Amer. Meteor. Soc., 84, 1205–1217.
doi: http://dx.doi.org/10.1175/BAMS-84-9-1205

5

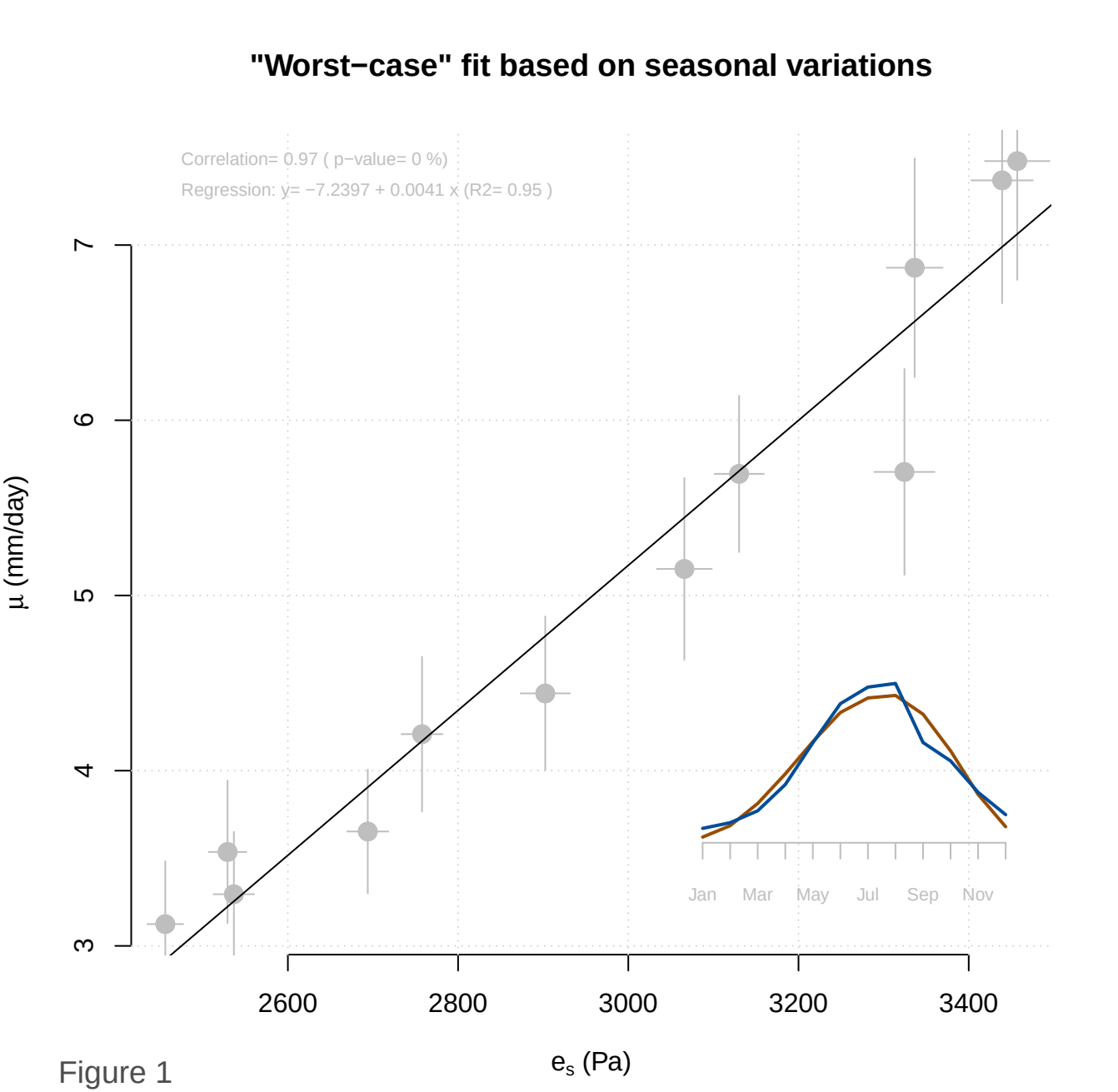

Figure 1

VELIKIE LUKI (30.62E/56.35N; 97m.a.s.l.)

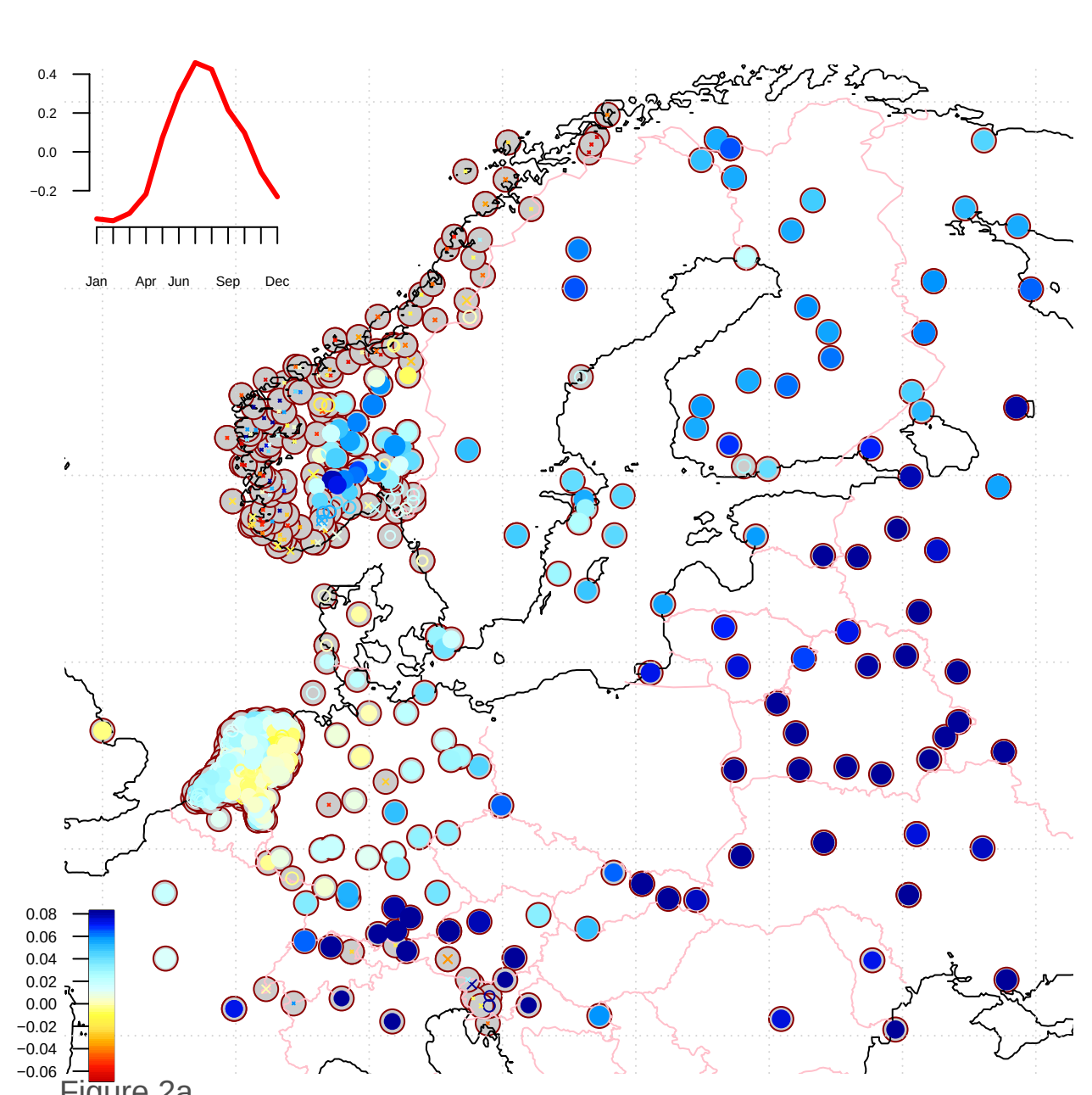

Figure 2a

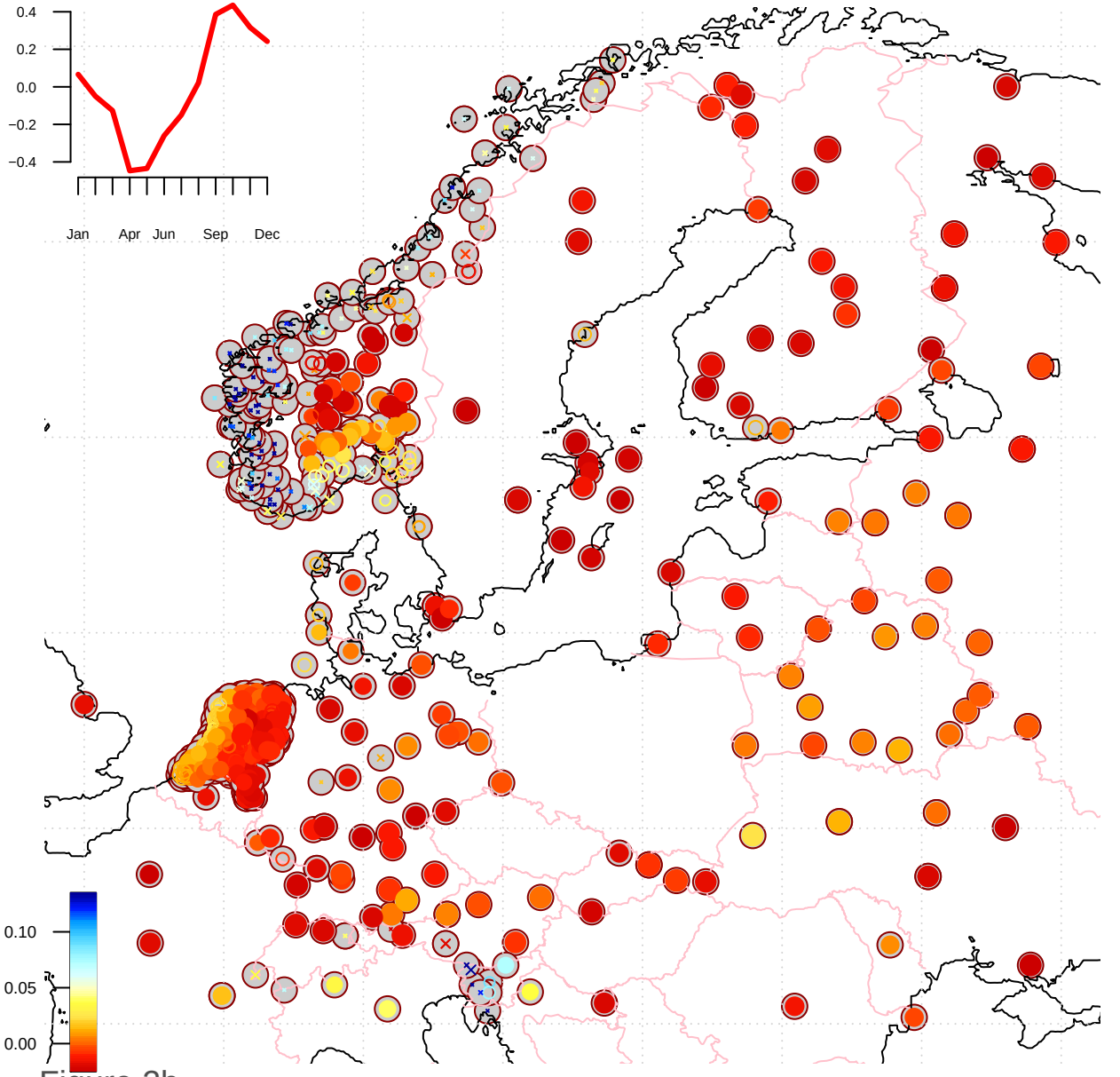

Figure 2b

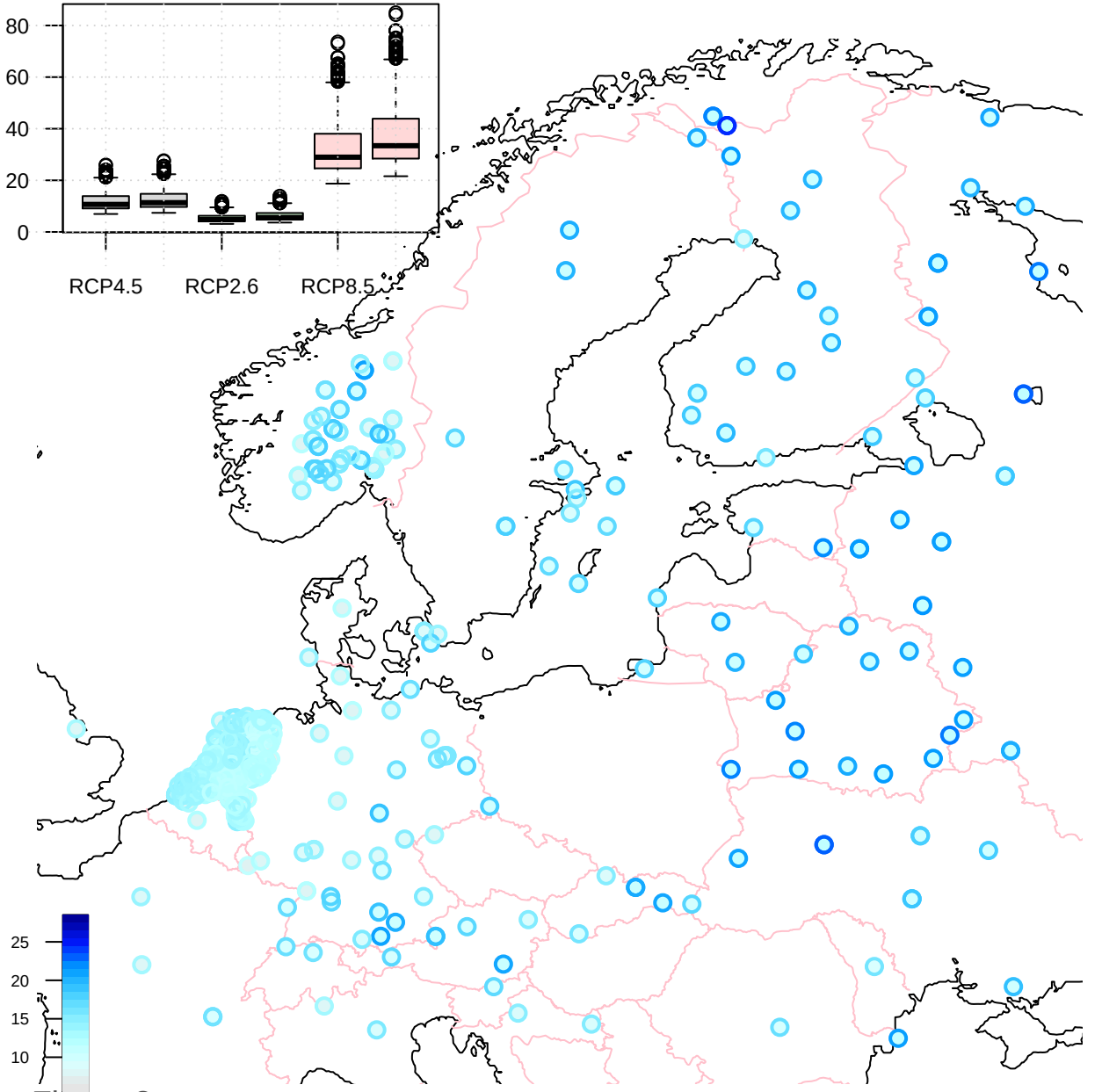

Figure 3